NAVIER-STOKES COMPUTATIONS ON A LAMINAR AIRFOIL

Erkki Soinne, Royal Institute of Technology and Saab AB, Sweden

Presented at XXV OSTIV Congress, Saint-Auban, France

ABSTRACT

The aim of this paper is to answer the question: what is the state of the art when analyzing a low speed laminar airfoil with a modern Navier-Stokes program. As a test case the well-known airfoil FX 61-163 has been chosen. Two turbulence models of the program NS2D are used; a two-layer k-ε model and a modification of it with an eddy viscosity limiter. A total of 111 one- night computer runs are included into this report. The computed values of lift, drag and pitching moment coefficients are compared with existing wind tunnel data as well as results from MSES program.

INTRODUCTION

There has been an increasing amount of research in the numerical solution of Navier- Stokes equations in the past decade. However, the main effort has been directed towards commercial and military aviation where the flows are mainly turbulent due to high Reynolds numbers. The objective of this paper is what level of precision can be obtained on the dimensionless coefficients defining the airfoil performance, the lift coefficient c_L, drag coefficient c_D and moment coefficient $c_{m.25}$? The lift and drag coefficients constitute the airfoil polar. The moment coefficient is needed for the determination of the trim drag, because the pitching moment must be balanced with a tail load on a complete aircraft.

The test airfoil should be a typical example of well known airfoils that have been used in practice. Here the classical laminar airfoil FX 61-163 designed by F.X. Wortmann has been chosen. This is an unflapped single-element airfoil with a thickness ratio of 16.3% that has been used on several gliders, for example on ASW-l9. The airfoil represents the first generation of laminar airfoils designed for the Reynolds numbers in question for gliders, say Re=0.5...3.0·10⁶.

Due to the extensive computing times required a Navier-Stokes code is not the obvious choice for analyzing a laminar airfoil. Here the question is rather seen the other way round. A low Reynolds number laminar airfoil gives a complementary test case for a code, which should be able to give good results in any arbitrary flow case.

WIND TUNNEL TESTS

The FX 61-163 airfoil has been tested in the laminar flow wind tunnel at the Technical University of Stuttgart (reference 2) and later on at the Tehnical University of Delft (reference 3). There is also a third measurement carried out at the University of Alberta in Canada (reference 5). The original OSTIV paper (reference 8) contains a discussion on the different measurements that are presented together with the computations in figure 6.

Figures 7 and 8 show together with computations measured lift curves and drag polars, when contamination with insects has been simulated with turbulator tapes at the airfoil nose, see measurements by Althaus in reference 1.

NS2D PROGRAM

The Saab Navier-Stokes code NS2D solves the two-dimensional time-dependent compressible Reynolds averaged Navier-Stokes equations written in conservative form. The equations are solved in a structured multiblock domain. However, in this work only a single block mesh was used. The mean flow equations are discretized in space using a cell-centered finite volume approximation. A blending of adaptive second and fourth order artificial dissipation terms are added to the numerical scheme to damp spurious oscillations and improve convergence. The mean flow equations are integrated in time using an explicit five-step Runge-Kutta scheme. Local time steps as well as multigrid technique are available for convergence acceleration. The far-field boundary velocities are corrected based on the circulation Γ which is obtained from a user specified lift coefficient. The airfoil lift and drag are determined by integration of airfoil surface pressure p and wall stress $τ_w$.

The code is intended primarily for the analysis of commercial and military airplanes where the flows are mainly turbulent and often separated. In the version used for this work there was no transition model available why the transition locations had to be specified explicitly. The code has been validated in BRITE/EURAM EUROVAL and GARTEUR collaboration projects with applications such as Aerospatiale A airfoil, NLR7301 flapped airfoil and Airbus A310 three element airfoil. At Saab, the code has been used for example for the computations of Saab 2000 wing flap and horizontal tail.

In this study the two-layer turbulence model, based on the Launder-Jones k-ε model, was used. Wolfshtein's one-equation model was adopted near the wall. Computations were also made with a modified turbulence model taking into account the shear stress transport. The turbulence models and the governing equations are described in the original paper, reference 8.

At the airfoil surface, no-slip and adiabatic wall conditions are assumed while the far-field boundary conditions are based on the one-dimensional Riemann invariants combined with a velocity correction. The correction velocities are based on the circulation Γ, which is obtained from the computed lift coefficient c_L. This velocity correction allows the far-field boundary to be placed closer to the airfoil without degrading the solution accuracy. By choosing the circulation Γ = 0 the usual Riemann invariants based on free stream values are recovered.

COMPUTATIONS WITH NS2D

Computation procedure

The mesh for the computations was created by an in-

house program at Saab. The created C-mesh has 64 cells perpendicular and 256 cells parallel to the airfoil surface. The airfoil trailing edge ends in a single point having thus zero thickness as shown in the grid in figure 1. To guarantee a sufficient resolution in the viscous sublayer of the boundary layer the grid was generated so that the distance from the airfoil contour to the first cell center should satisfy the condition y+< 1 where the dimensionless wall normal distance is defined as

$$y^+ = \rho \frac{u_\tau}{\mu} y_n \qquad (1)$$

and u_τ is the friction velocity

$$u_\tau = \sqrt{\frac{\tau_w}{\rho}} \qquad (2)$$
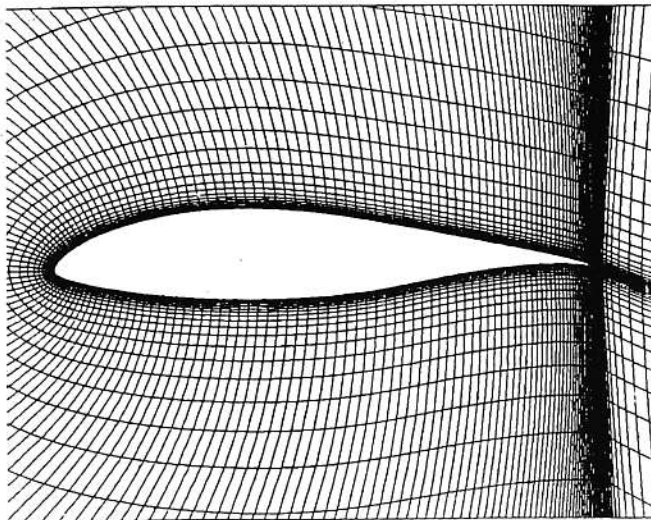
Figure 1: *A close-up view of the used mesh.*

This gave a first cell height in the order of $10^{-5}c$.

Four sets of computations were performed in this study:
- smooth airfoil, Re=1.5·10⁶, two-layer turbulence model
- transition fixed, Re=1.0·10⁶, two-layer turbulence model
- transition fixed, Re=2.5·10⁶, two-layer turbulence model
- smooth airfoil, Re=1.5·10⁶, modified two-layer turbulence model

The transition locations for the smooth airfoil were taken from the wind tunnel measurements of reference 2 shown in figure 6, because there was no transition model available in 1995-96 when the calculations were performed. The computations were started with the smooth airfoil at angle of attack α=4° well inside the laminar bucket. First the laminar flow case was solved for this angle of attack. Then the turbulence model was triggered and finally the turbulent flow was solved with a large number of iterations. The number of work units (iterations on the fine mesh level) was selected as 9000 which gave a run time of 13.5 hours on the SGI Indigo R4000 -workstation with a 32Mb RAM. As is seen in figures 2 and 3 the used 9000 work units were sufficient for convergence of the density residual and pressure lift coefficient c_{l_p} when using the two-layer turbulence model. The lift coefficient changed slowly in the third decimal during the latter half of iterations. The notches at the beginning of convergence are due to changes between the three used multigrid levels.

A measure on the solution accuracy is the distribution of total temperature, which should be constant in the entire flow field with adiabatic wall conditions. Figure 4 shows that the total temperature is constant except in the close vicinity of the airfoil contour. In theory there are total pressures losses in the boundary layer and wake which is confirmed in Figure 5. Further on the solutions proceeded in increasing and decreasing direction of angle of attack using the previously obtained turbulent flow solution as an initial state for the new angle of attack solution.

The transition locations of the airfoil with turbulator tapes of R°eference 1 had to be estimated by judgement, because the bumps in the tapes cause wedge shaped disturbances that successively force the boundary layer to become turbulent. The transition locations were set on the upper surface at 0.5 % and on the lower surface at 1.0 % chord. The solutions at Re=1.0·10⁶ with transition fixed were solved first by using the solutions of the smooth airfoil at corresponding angles of attack as initial values. The solutions were then used as initial conditions for the computations at Re=2.5·10⁶.

The modified turbulence model was used to study the airfoil stall. The initial solution was taken at α=5° from the smooth airfoil computations with the basic two-layer turbulence model. Then the angle of attack was successively increased. The iterations were continued until the change in lift coefficient was less than 1.0 % of its value. This showed to lead with the modified turbulence model in iteration numbers up to 54000 work units. The logarithm of the rms value of density reached the value -7.2 during the first run as in figure 2, but was then virtually unchanged although the pressure lift coefficient slowly converged during the successive runs.

Aerodynamic coefficients

The computed lift curves, drag polars and moment coefficients are presented in figures 6, 7 and 8 and the numerical values are found in reference 7. The smooth airfoil polar is computed using the two-layer turbulence model at Reynolds number 1.5·10⁶. As shown in figure 6 the lift curve slope is approximately 5 % higher than the measured reference curve. In the computed values there is also a shift of roughly 0.5° in the zero lift direction. Consequently the computed lift co-efficient values are around 0.08 higher than the measured ones in the linear lift range. This is rather surprising since the code has usually produced quite accurate lift predictions in attached flow conditions.

The computations with transition fixed aft of the leading edge show that the lift curves have been lowered due to a thicker boundary layer, see figures 7 and 8. However the curves are still above the measured ones in the same way as for the smooth airfoil.

The two-layer turbulence model does not produce a complete stall up to the highest angle of attack studied α=16°, but the lift curve continues to rise. The modified turbulence model gives a maximum lift coefficient $c_{l_{max}}$ =
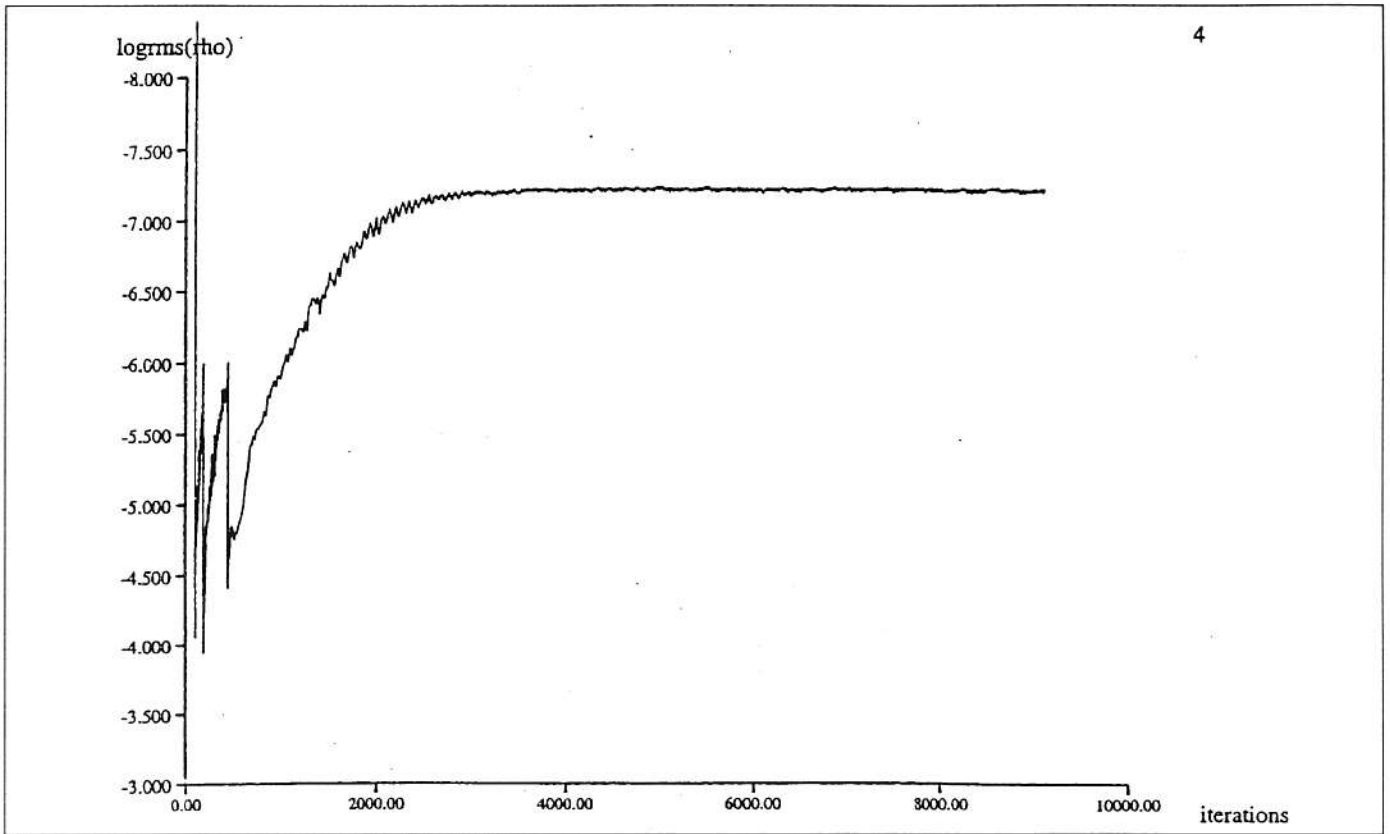
Figure 2: *Convergence of density residual, FX 61-163 smooth airfoil, $\alpha=4°$, Re=1.5·10⁶.*
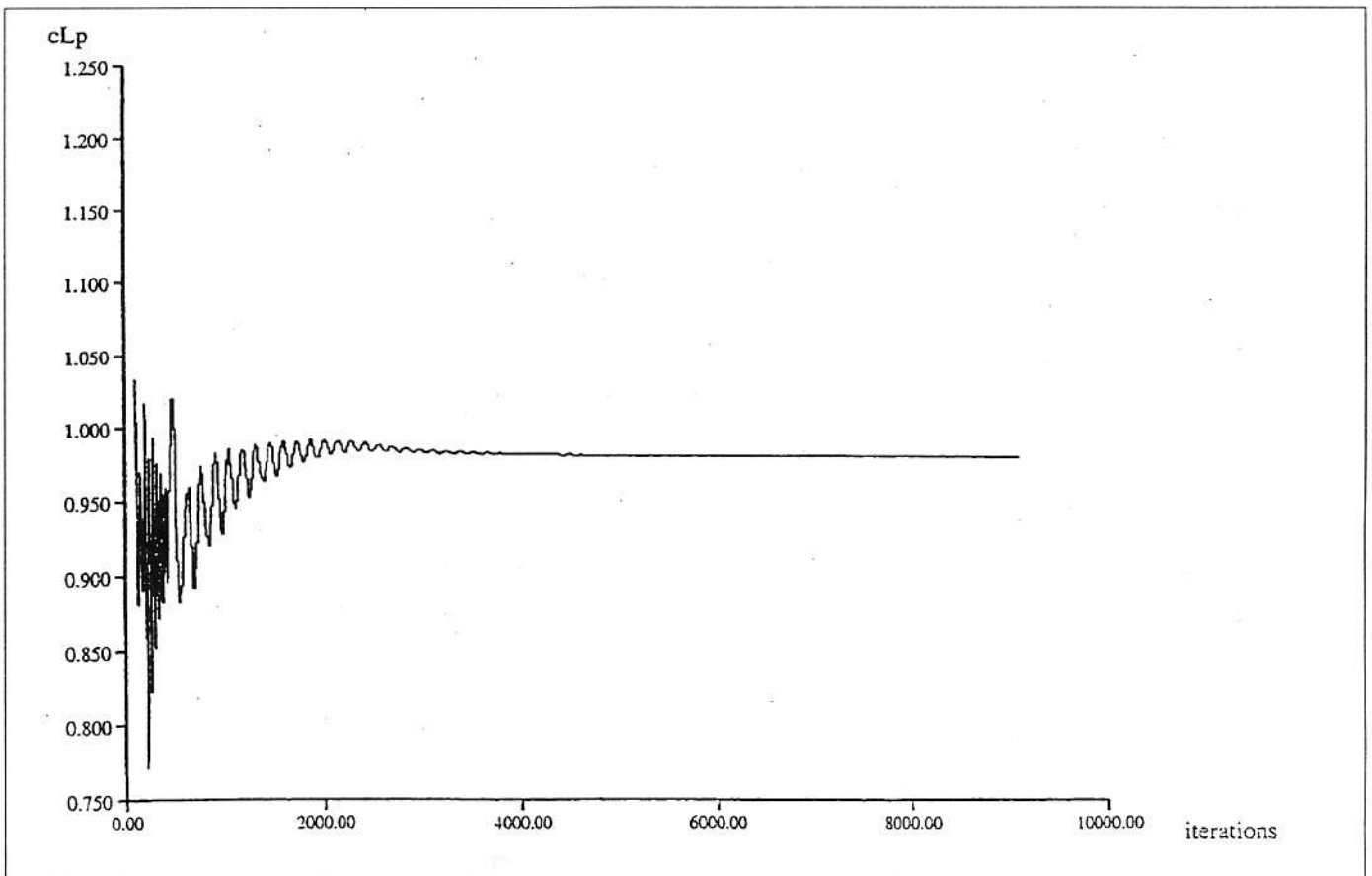
Figure 3: *Convergence of pressure lift coefficient, FX 61-163 smooth airfoil, $\alpha=4°$, Re=1.5·10⁶.*
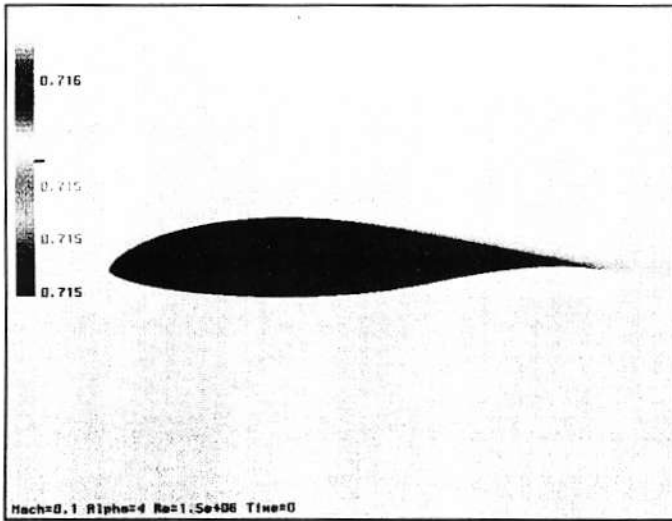
Figure 4: Distribution of total temperature, FX 61-163 smooth airfoil.
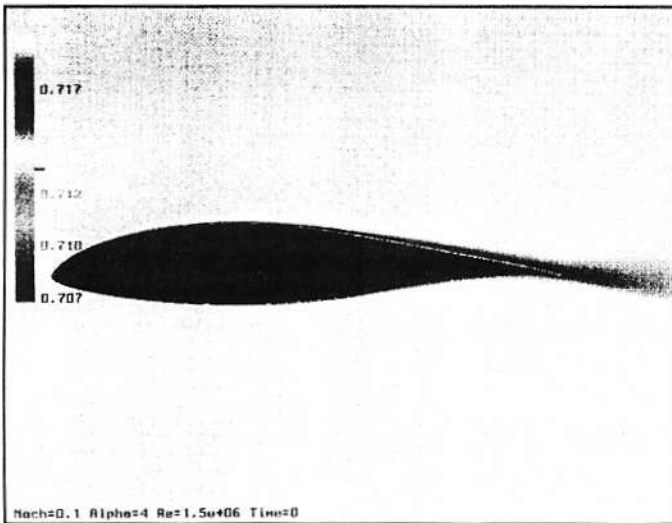
Figure 5: Distribution of total pressure, FX 61-163 smooth airfoil.

1.715 at angle of attack $\alpha=13°$. The corresponding measured values are $c_{L_{max}} = 1.379$ $\alpha=11°$. The modified model tries to follow the measured curve already at an angle of attack of $\alpha=7°$, but fails to produce more than a local kink in the lift curve.

The drag polar for the smooth airfoil, computed with the basic two-layer turbulence model at Reynolds number $1.5\cdot10^6$ is shown in figure 6. For the smooth airfoil the computed drag coefficients in the laminar bucket somewhat too high varying in the interval $\Delta c_D = 0.0005\ldots0.002$. This means that the computed values are 7 to 20 % higher than the measured ones. The form of the laminar bucket is computed fairly well even at the edges of the bucket.

The computations with transition fixed aft of the leading edge are shown in figures 7 and 8. The drag polars show a considerable increase in drag compared with the smooth airfoil values. Comparison with measured values is not straightforward because the applied turbulator tapes seem to have been partially insufficient in the wind tunnel tests. Notice that the measured drag at low angles of attack is clearly lower for the lower Reynolds number test. It seems that the flow in the tests has been fully turbulent only in the vicinity of the laminar bucket upper edge. In this area the computed drag has been, say $\Delta c_L = 0.002$ higher than the measured values. The difference between measurements and computations was roughly the same at $Re=2.5\cdot10^6$. Because the two-layer turbulence model fails to predict the airfoil stall the form of the drag bucket at the upper edge is not reproduced very well.

Initial runs revealed a program error in the calculation of the pitching moment coefficient, which was corrected. The moment coefficients for the smooth airfoil at Reynolds number $1.5\cdot10^6$, computed with the basic two-layer turbulence model, are depicted in figure 6. For the smooth airfoil, the computed moment coefficient curve shows a similar form as measured in Stuttgart. The absolute values are somewhat higher, $\Delta c_{m.25}=0.02$, which is roughly 20 % of the measured value. It is logical that, with computed lift coefficients exceeding the measured values, the computed moment coefficients show more negative values than the measured ones and the deviation is due to the flow conditions mainly at the airfoil trailing edge. The moment coefficients for the airfoil with transition fixed aft of leading edge at Reynolds number $2.5\cdot10^6$ shows only small differences compared with the transition free case. The numerical results are not shown here but are found in reference 7.

Distributions

A color plot of the velocity distribution in the flow field around the smooth airfoil at angle of attack $\alpha=4°$ is shown in figure 9 (the resolution is better in the original color picture of reference 8). The solved flow field seems to be smooth and shows boundary layer growth towards the airfoil trailing edge. Figure 10 shows a close-up view of the velocity in the airfoil wake revealing a vague trace of the mesh manifesting itself as a slightly darker area below the wake. A corresponding distribution on pressure coefficient C_p shows that the static pressure in the boundary layer is the same as in the outside main flow, see figure 11. The distribution of the kinetic energy in the airfoil boundary layers and wake is shown in figure 12. The distribution seems to be biased strongly on the upper side of the wake but due to the logarithmic scale this is mainly a numerical effect.

In figure 13, computed pressure coefficients of the nominal airfoil are compared with the measurements of the sailplane wing model at Delf at angles of attack 2 and 6 degrees. Two differences can be noticed. The computations show a larger ΔC_p in the vicinity of the airfoil trailing edge than the measurements. This will contribute to an increased lift coefficient and a more negative moment coefficient. One reason for this may be the finite trailing edge thickness of the model. Hence the effect of finite thickness on the computed results should be investigated. Also a general refinement of the mesh should be studied to check that used mesh has been sufficiently fine. It seems that the cambered trailing edge of the airfoil has posed a demanding case for the computer code. The other differ-
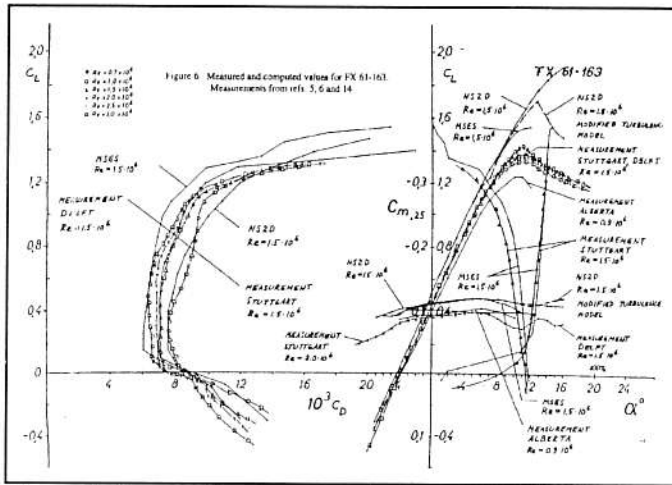
Figure 6: *Measured and computed values for FX 61-163. Measurements from references 5, 6 and 14.*

Figure 7: *Lift curve and drag polar transition fixed aft of leading edge, Re=1.0·10⁶.*
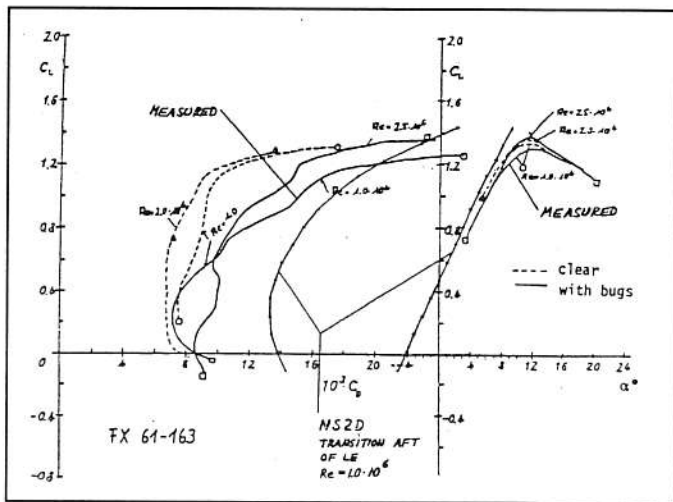
Figure 7: *Lift curve and drag polar transition fixed aft of leading edge, $Re=1.0 \cdot 10^6$.*
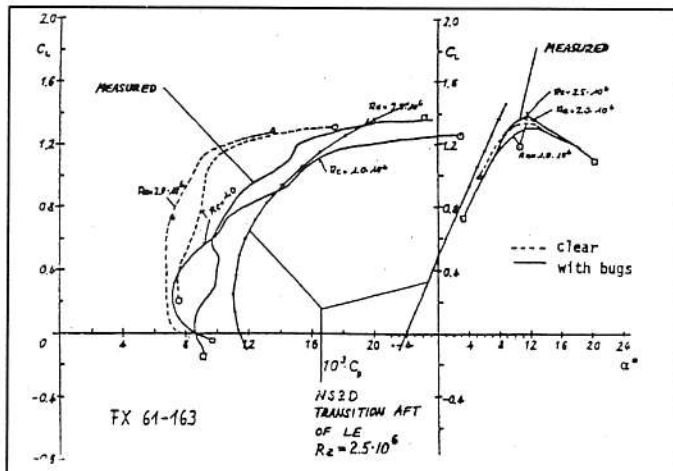
Figure 8: *Lift curve and drag polar transition fixed aft of leading edge, $Re=2.5 \cdot 10^6$.*

ence in the pressure coefficient distributions is that the measured curves show separation bubbles on both airfoil sides but these are lacking in the computed results. The missing of the bubble effect on the pressure coefficient

distributions may contribute to the obtained lift coefficient values. The notches and other differences in the pressure coefficient distributions may be due to differences in the measured versus computed airfoil contours.

Study now the results with the modified turbulence model. The maximum lift coefficient was attained at the angle of attack α=13°. At this angle of attack the computed skin friction coefficient distribution showed only a very small area of separated flow in the vicinity of the airfoil trailing edge. There was no sign of leading edge separation. Hence even the modified turbulence model fails to predict correctly the successively increasing flow separation. Corresponding, chordwise distribution in the poststall area at α=16°, not shown here, revealed that a flow separation then covers the airfoil upper surface from 45 % chord to the trailing edge. The form of the stream-lines in this flow case, shown in figure 15, confirms that there is a considerable area of separated flow.

COMPUTATIONS WITH MSES

MSES is a computer program, developed at MIT by Mark Drela (reference 4), for the analysis and design of
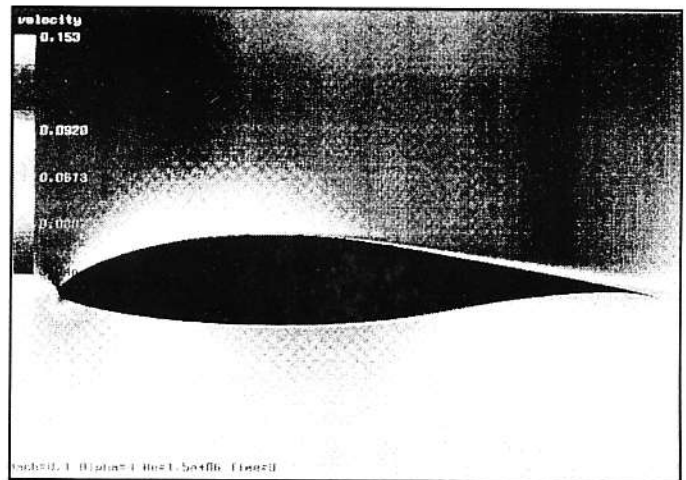
Figure 9: *Velocity distribution, FX 61-163 smooth airfoil.*
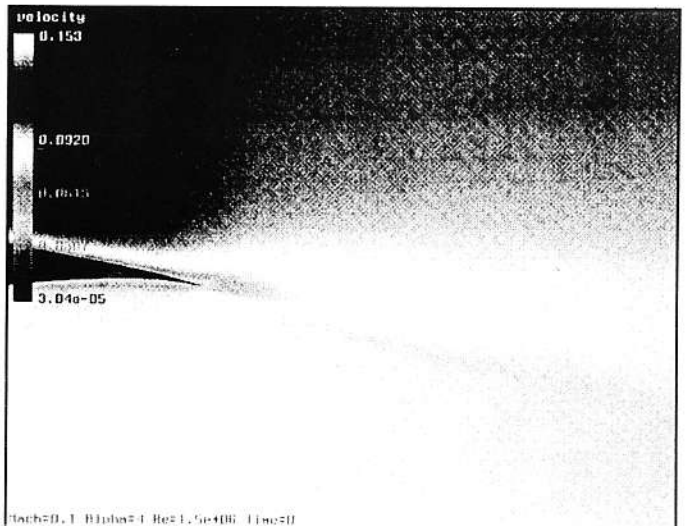
Figure 10: *Velocity distribution, FX 61-163 smooth airfoil wake.*
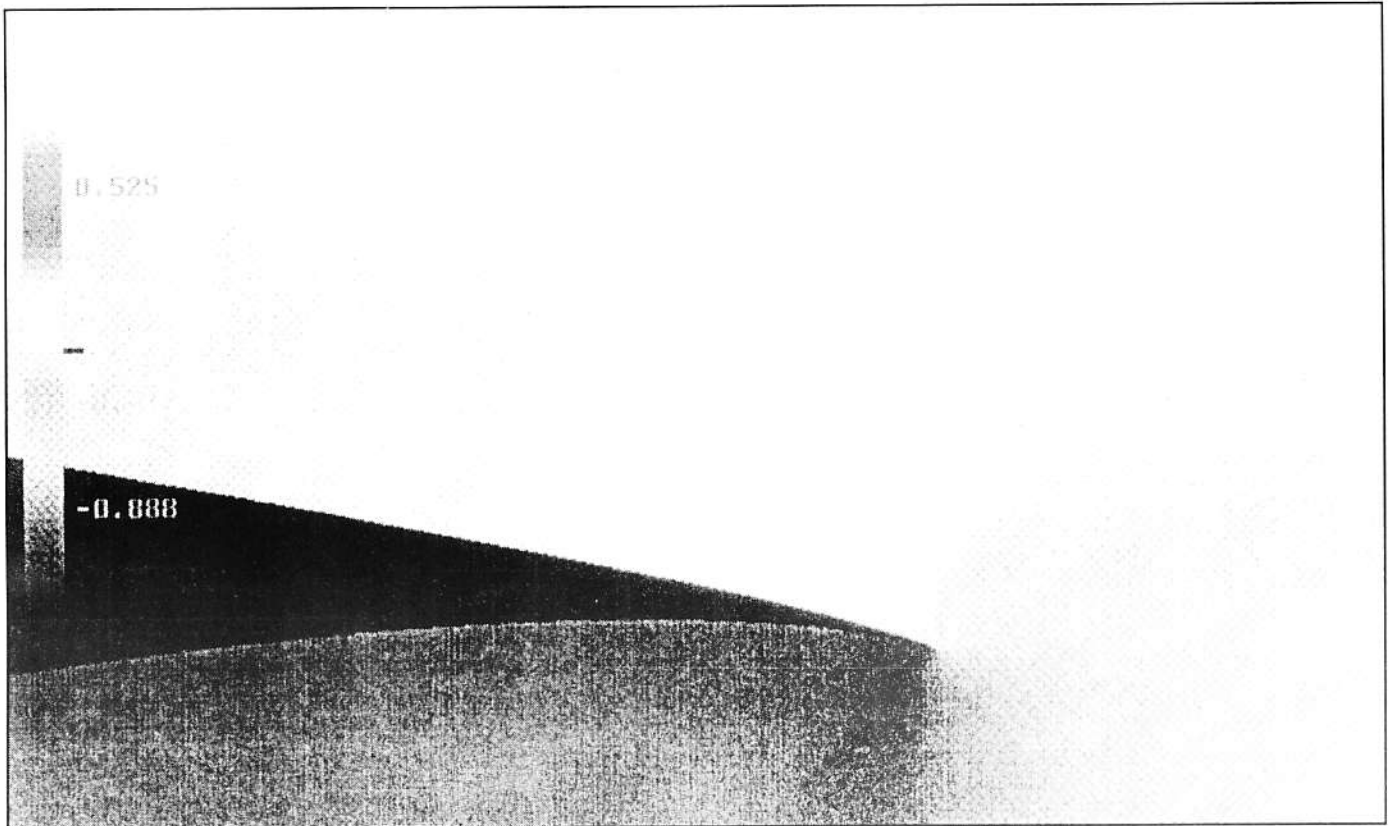
Figure 11: Pressure coefficient distribution at FX 61-163 smooth airfoil trailing edge.
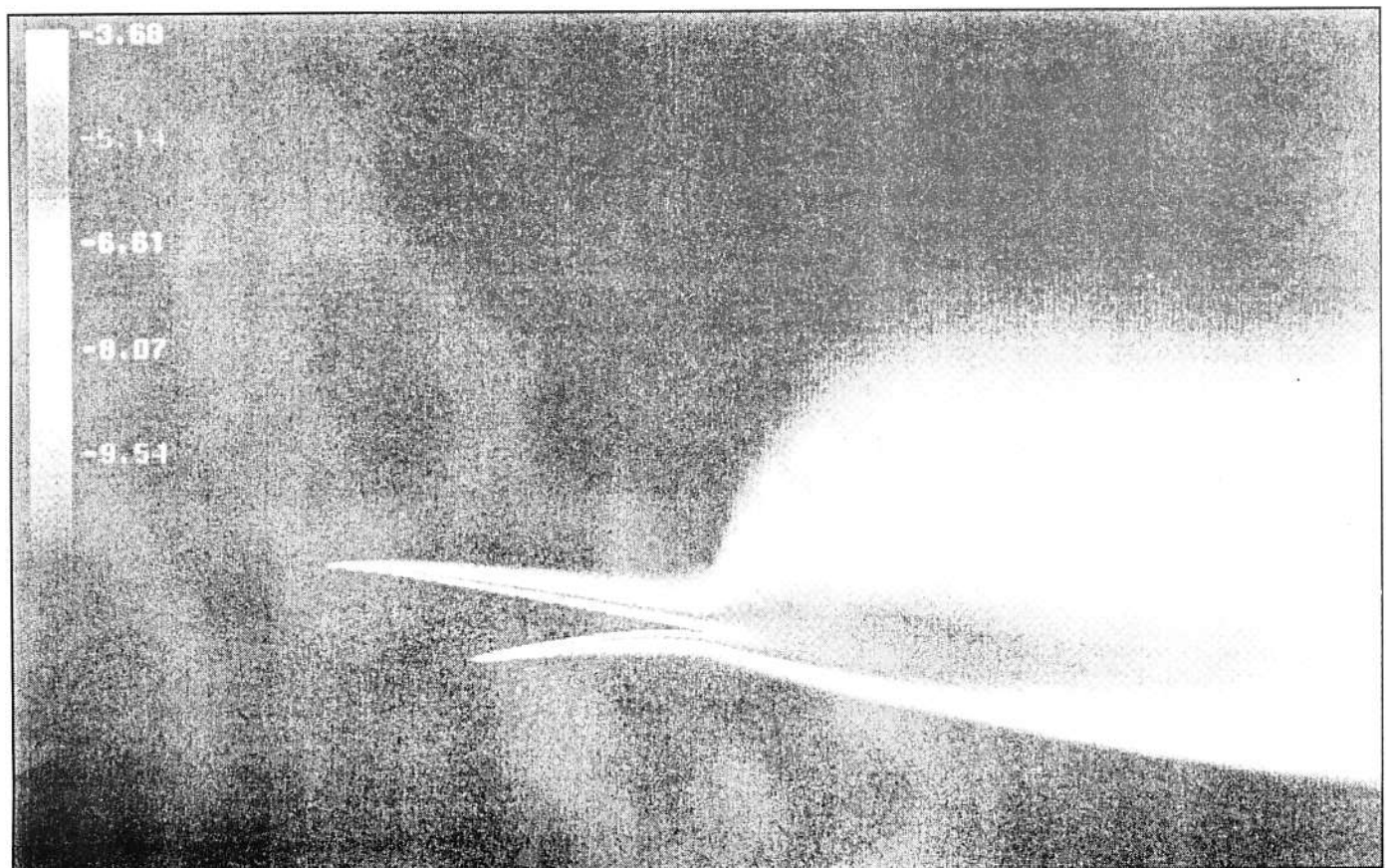
Figure 12: Distribution of kinetic energy on logarithmic scale, FX 61-163 smooth airfoil.
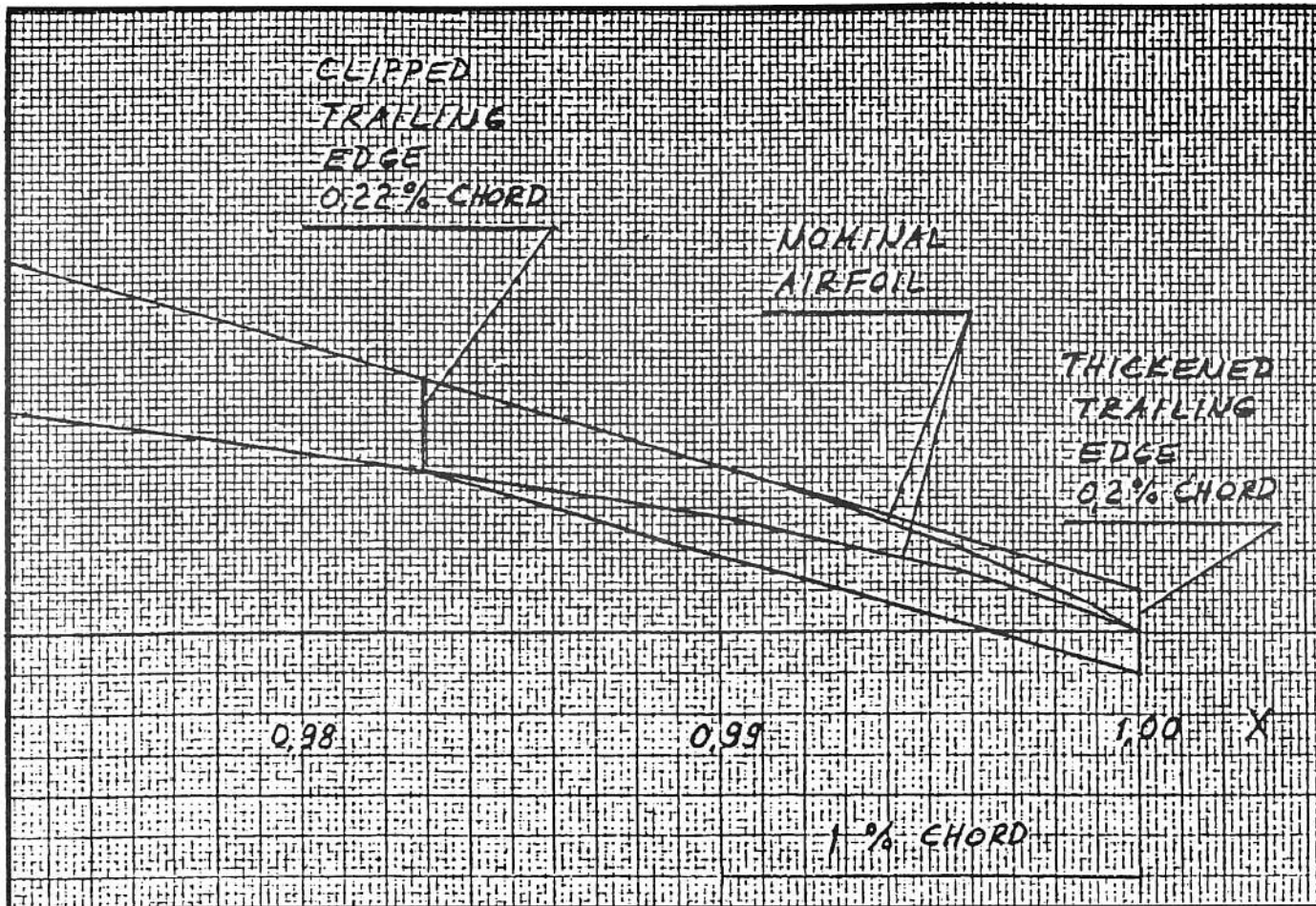
Figure 13: *Close-up view of the airfoil trailing edge modifications.*
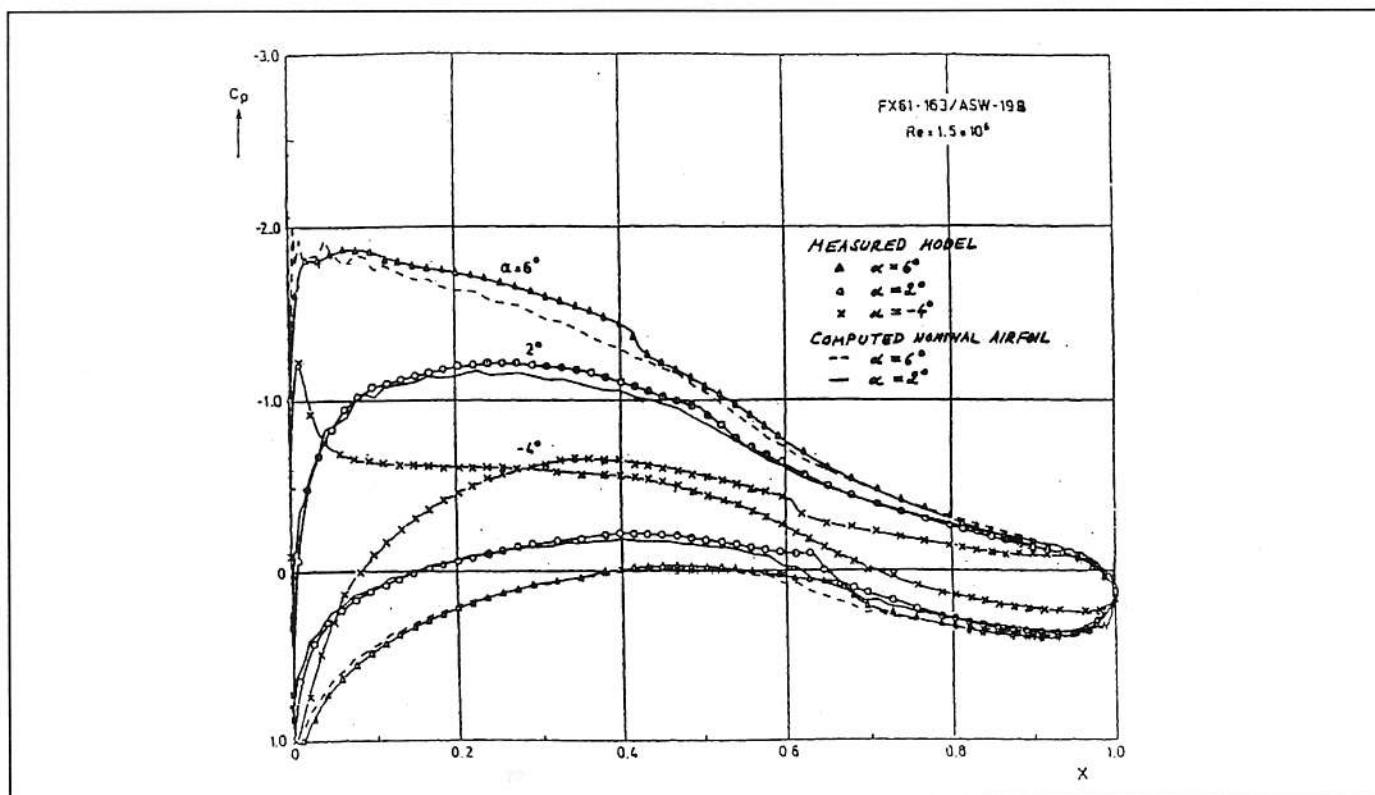
Figure 14: *Computed and measured (Ref. 3) pressure coefficient distributions.*
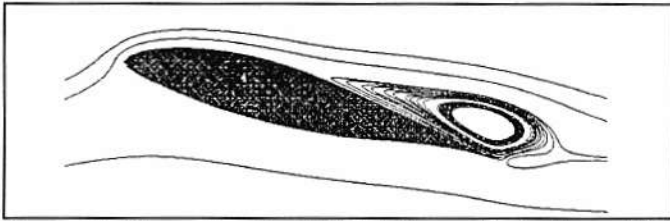
Figure 15: Streamlines for FX 61-163 smooth airfoil, modified turbulence model.

two-dimensional transonic airfoils and cascades. It uses Newton method to solve the Euler equations on an intrinsic streamline grid coupled with integral boundary layer equations. The coupling procedure gives stable convergence for flows with limited separation regions. For laminar boundary layer, Drela has derived a two-equation method based on Falkner-Skan velocity profiles. A transition criterion based on the Orr-Sommerfeld equation has been developed and applied to transitional separation bubbles. For the turbulent boundary layer a two-parameter velocity profile has been developed based on Swafford's analytic expression and a formula for dissipation coefficient based on equilibrium boundary layer with a correction due to upstream flow history. In the wake the turbulent boundary layer equations are used by setting the skin friction coefficient to zero.

Because the lift curve computed with NS2D deviated from the wind tunnel measurements more than expected, calculations with MSES were done for comparison. Three sets of calculations were performed at $Re=1.5 \cdot 10^6$:

- FX 61-163 nominal airfoil
- FX 61-163 with trailing edge thickened to 0.2 % of chord
- FX 61-163 with trailing edge clipped to a thickness of 0.22 % of chord

The three trailing edge geometries are shown in figure 15. The computational grid was generated for the airfoil at zero angle of attack using the default values of the program and just performing an elliptic smoothing (also a default option). The computations proceeded with an interval of $\Delta\alpha=0.5°$ towards the edges of the laminar bucket. At $\alpha=10°$ the run halted due to convergence problems and a new grid was generated. In the supplementary run the angle of attack was increased with a step of 0.1°. All runs were performed with the default value of n=9.0 on the amplification factor for the en transition model.

The computed drag polar, lift and moment curves, and transition locations for the nominal airfoil are shown in figure 6 together with the wind tunnel measurements. The lift curve shows the same results as with NS2D of yielding a slope of 5% higher than the measurements. The lift coefficients in the linear range are on average 0.08 higher than the measured values. The computed maximum lift coefficient exceeds the maximum measured value by $\Delta c_L = 0.17$ at almost same angle of attack as in the measurements. The computed values on the pitching moment coefficient are practically the same as with NS2D. The absolute values of the moment coefficient are 0.02 higher than the mea-

sured values. The numerical values of the computed results are presented in reference 6.

In the laminar bucket the computed drag coefficient is 9...17% lower than the values in the wind tunnel tests. The form of the laminar bucket is produced fairly well but values at the upper edge seem to be somewhat optimistic (the bucket is slightly too wide). The reason for too low drag coefficients is connected to the prediction of transition location. As is seen in figure 6 MSES predicts the transition especially on the airfoil upper surface somewhat (say 5% chord) too far downstream. Although the drag due to laminar separation bubbles is taken into account the program produces somewhat too low values on the airfoil profile drag.

The thickening of the airfoil trailing edge had only a marginal effect on the lift curve and moment coefficient as shown in figure 16. The clipped trailing edge produced considerably less lift and pitching moment. The lift curve follows fairly well the measured curve in the linear range but the lift curve slope is 5 % higher than in the measurements. The maximum lift coefficient value is reduced but is still $\Delta c_L = 0.07$ above the measured one. Also the absolute value of the pitching moment is significantly reduced and matches well the measured values. The drag coefficients in the laminar buckets are virtually unchanged but the buckets have followed the shift of the lift curves.

The computations on the trailing edge modifications show that even small changes at a strongly cusped trailing edge have a significant effect on the lift and pitching moment coefficients. This may be a major explanation for the differences in the computed and measured results, as the true trailing edge geometry of the wind tunnel models, is not known.

CONCLUSIONS

The performed runs with the Navier-Stokes code NS2D show that computation of a complete airfoil polar is needed for insight into the overall performance of the program. An error in the computation of pitching moment coefficient was detected and corrected. The drag and the form of the laminar bucket is reproduced with fairly good precision for the smooth airfoil. The Launder/Jones two-layer turbulence model fails to predict the airfoil stall. The modified turbulence model shows encouraging improvement in stall prediction but the maximum lift coefficient is still too high. MSES gives a better estimate on the maximum lift coefficient but NS2D predicts the form of the laminar bucket slightly better. (On multi-element airfoils with separated flow NS2D has in our experience been superior both on lift and drag).

The chosen airfoil FX 61-163 is a demanding test case. Due to the strongly cusped trailing edge the flow is sensitive to small changes in the trailing edge geometry. NS2D and MSES give the same results on the nominal airfoil lift curve in the linear range. The wind tunnel tests show less lift which can be explained by a finite trailing edge thickness in the tests. Detailed studies with the exact model geometry and refined grids should be carried out to con-
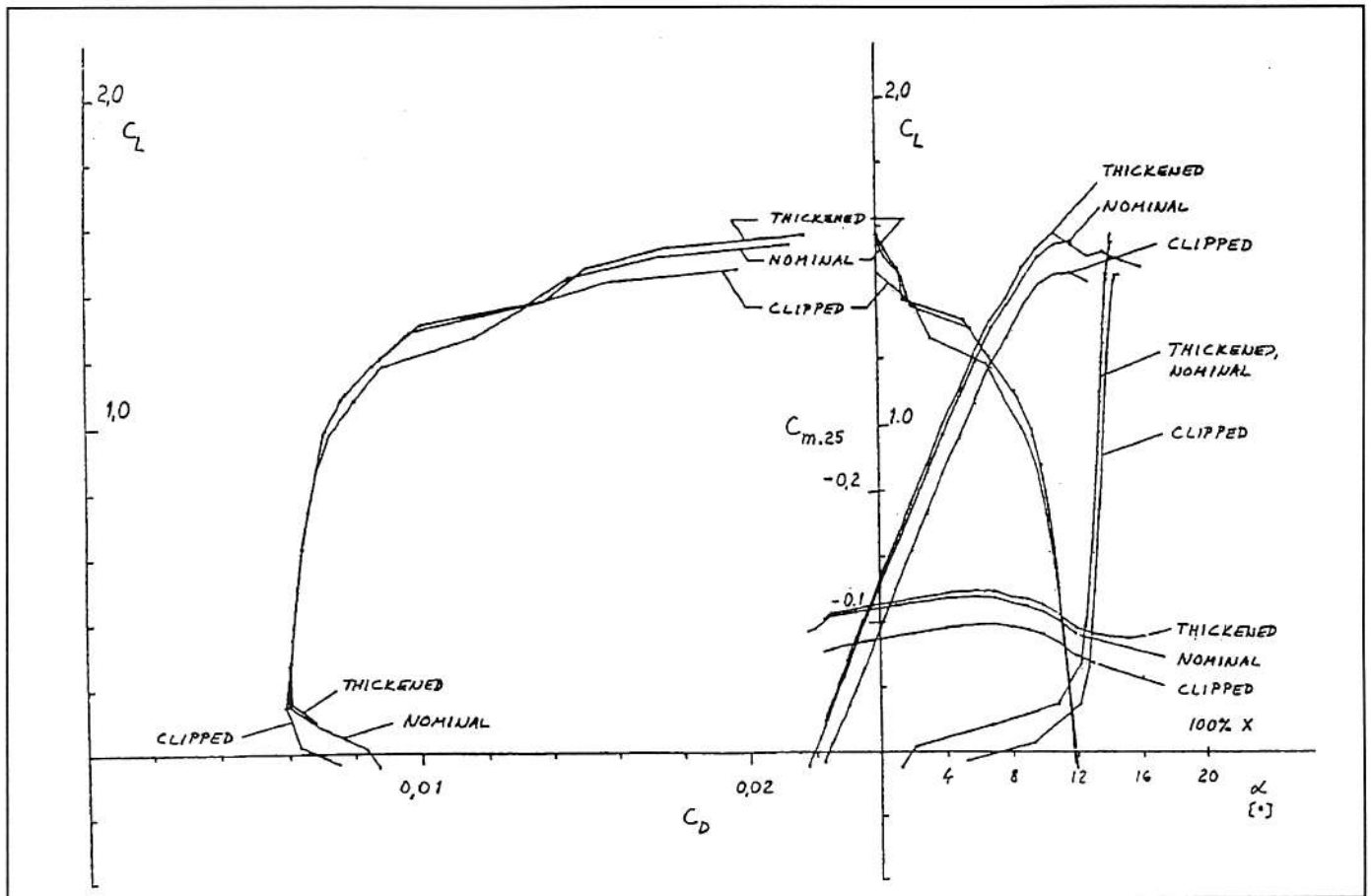
Figure 16: *Effect of trailing edge modifications at Re=1.5·10⁶.*

firm the differences. The effect of the flow conditions at the trailing edge on the pitching moment is even stronger due to the large moment arm. The same will be true also for the hinge moment of an airfoil control surface or flap, so a careful modeling of the grid would be needed.

REFERENCES

1. Althaus D., Influencing Transition on Airfoils, Technical soaring, December 1981, p.82...93.
2. Althaus D., Stuttgarter Profilkatalog I, Institut fur Aerodynamik und Gasdynamik der Universitat Stuttgart, 1972, 386 p.
3. Boermans L.M.M., Selen H.J.W., On the design of some airfoils for sailplane application, Delft University of Technology, Department of Aerospace Engineering, April 1 981, 48 p.
4. Drela M., A User's guide to MSES 2.7, MIT Computational Aerospace Sciences Laboratory, November 1994, 28 p.
5. Marsden D.J., Wind Tunnel Tests of a Slotted Flapped Wing Section, Canadian Aeronautics and Space Journal, Vol. 24 No. 2, March/April 1978, p. 83...91.
6. Soinne E., Analysis of FX 61-163 Airfoil with MSES Program, Royal Institute of Technology, Department of Aeronautics, Report No. 97-3, 44p.
7. Soinne E., Evaluation of Navier-Stokes program NS2D for a low speed airfoil, Royal Institute of Technology, Department of Aeronautics, Report No. 97-2, 53 p.
8. Soinne E., Navier-Stokes Computations on a Laminar Airfoil, XXV OSTIV Congress, 1997, 26 p.